

Dimensional crossover of thermal transport in quantum harmonic lattices coupled to self-consistent reservoirs

Kiminori Hattori  and Masaya Sambonchiku

Department of Systems Innovation, Graduate School of Engineering Science, Osaka University, Toyonaka, Osaka 560-8531, Japan



(Received 14 March 2020; accepted 19 June 2020; published 8 July 2020)

In this study, we investigate thermal transport in d -dimensional quantum harmonic lattices coupled to self-consistent reservoirs. The d -dimensional system is treated as a set of Klein-Gordon chains by exploiting an orthogonal transformation. For generality, the self-energy that describes the reservoir-system coupling is assumed to be a power function of energy $\Sigma \propto -i\varepsilon^n$, where n is limited to odd integers because of the reality condition. Total momentum conservation is violated for $n = 1$ but otherwise preserved. In this approach, we show that for $n = 1$, thermal conductivity remains finite in the thermodynamic limit and normal transport takes place for an arbitrary value of d . For $n = 3, 5, 7, \dots$, however, thermal conductivity diverges and thermal transport becomes anomalous as long as $d < n$, whereas normal transport is recovered when $d \geq n$. These criteria derived for quantum-mechanical lattices imply that normal transport emerges in high enough dimensions despite total momentum conservation and reinforce the prevailing conjecture deduced in the classical limit.

DOI: [10.1103/PhysRevE.102.012121](https://doi.org/10.1103/PhysRevE.102.012121)

I. INTRODUCTION

It is conventional to expect that heat conduction follows Fourier's law, which relates heat current to a temperature gradient as $\mathbf{J} = -\kappa \nabla \theta$, where κ is the material-dependent thermal conductivity. Because of energy conservation, this law predicts a linear temperature profile for a small temperature bias along the direction of heat flow in the steady state. It also follows that for a fixed temperature bias $\Delta\theta$, the heat current varies as $J \propto L^{-1}$, where L is the system size. In nonequilibrium statistical physics, it is a fundamental challenge to derive Fourier's law from first principles. This issue remains unresolved despite extensive theoretical studies thus far. From these studies, it is widely accepted at present that Fourier's law is genuinely broken in a low-dimensional lattice system without external forces that break total momentum conservation [1–5]. In particular, anharmonic Fermi-Pasta-Ulam chains and disordered harmonic chains are the typical examples showing this anomaly. For these systems, the finite-size thermal conductivity defined as $\kappa = JL/\Delta\theta$ diverges in the thermodynamic limit $L \rightarrow \infty$. Heat transport that disobeys Fourier's law is termed as anomalous transport to distinguish it from normal transport following this law.

The non-Fourier transport is observed experimentally in carbon and boron-nitride nanotubes [6] and in single-layer graphene [7]. In experiments, dimensional crossover of thermal transport is also explored in few-layer graphene [8].

In addition, it may be worth mentioning that the finite-size conductivity following Fourier's law is reported for a disordered harmonic chain with strong boundary mismatch between the system and the external heat reservoir [9,10]. The investigation of the relevant models may disprove the prevailing conjecture mentioned above if the normality is also verified for local temperatures. Apart from the unresolved issue for boundary-limited transport, in this article, we ad-

dress thermal transport in a lattice system without boundary mismatch.

A simple model that reproduces normal transport is a linear harmonic chain coupled to a self-consistent reservoir (SCR) at each site. In the SCR model, thermal transport is analyzed self-consistently under the adiabatic condition that no net energy current flows into each inner reservoir. The fictitious stochastic reservoir incorporates scattering and dephasing mechanisms into the system. This is parallel to the Büttiker probe used to mimic inelastic scattering in electron transport [11–13]. The classical version of this model was first studied by Bolsterli *et al.* [14,15], and exactly solved by Bonetto *et al.* [16]. They showed a linear temperature profile and a finite thermal conductivity obeying Fourier's law in the thermodynamic limit. However, the classical model is valid only in the high temperature limit, since it assumes the classical Langevin dynamics. The quantum version of the SCR model was first studied by Visscher and Rich [17] in terms of the quantum Langevin equation formalism. Subsequently, Dhar and Roy [18,19] derived the exact formula for a temperature dependent thermal conductivity in the thermodynamic limit. Recently, Hattori and Yoshikawa [20] extended this model to elucidate anomalous transport occurring in the quantum systems by introducing an inner reservoir that preserves total momentum conservation.

The SCR models mentioned above usually consist of a one-dimensional (1D) chain. The 1D setting may be deficient due to the following reason. It is implied from the previous studies based on the classical Langevin dynamics that the anomaly emerges generically in 1D and 2D whenever total momentum conservation holds and massless Goldstone modes persist [1–5]. For instance, momentum-conserving anharmonic lattices show a power-law divergence in 1D and a logarithmic divergence in 2D. However, such anomalies disappear in 3D despite total momentum conservation. Although

these observations in higher dimensions are verifiable in the classical limit, it is unclear how dimensional crossover takes place in quantum-mechanical lattices such as the quantum version of the SCR model.

The aim of the present study is to resolve this issue by exploring thermal transport in d -dimensional quantum harmonic lattices coupled to SCRs. The paper is organized as follows. In Sec. II, the d -dimensional system is treated as a set of Klein-Gordon chains by using an orthogonal transformation. The heat current flowing in each chain is formulated in the Landauer-Büttiker formalism. In Sec. III, we compare numerical results for two representative models of inner reservoirs that lead to total momentum conservation and nonconservation. Examining dimensional crossovers exhibited by these models, we derive an analytic formula for thermal conductivity in arbitrary dimensions and an explicit criterion for validating Fourier's law in the quantum systems. Finally, Sec. IV provides a summary.

II. THEORETICAL FORMULATION

Throughout this paper, we shall work in units where $\hbar = k_B = 1$. We consider a d -dimensional hypercubic lattice with nearest-neighbor harmonic interactions [4,16,21–23]. Each lattice site is labeled by the vector (l_1, l_2, \dots, l_d) , where $l_i = 1, 2, \dots, M_i$ for $i = 1, 2, \dots, d$. The heat flux is induced along a temperature gradient in the first direction $i = 1$. The temperature is assumed to be uniform from symmetry in the remaining $d - 1$ transverse directions $i = 2, 3, \dots, d$, on which periodic boundary conditions are imposed. Henceforth, we adopt the notations $j = l_1$ and $l = (l_2, l_3, \dots, l_d)$ for brevity. The length of the system is $N = M_1$. The cross section is defined as $M = \prod_{i=2}^d M_i$ for $d \geq 2$ and $M = 1$ for $d = 1$.

A scalar displacement q_{jl} of a particle from its equilibrium position obeys the equation of motion

$$\ddot{q}_{jl} + \sum_{j'l'} K_{jl;j'l'} q_{j'l'} = 0, \quad (1)$$

where the particle mass is taken as unity for simplicity. The force constant matrix is decomposed into $K_{jl;j'l'} = K_{jj'} \delta_{ll'} + K_{ll'}^\perp \delta_{jj'}$, where $K_{jj'} = t^2(2\delta_{jj'} - \delta_{j,j'+1} - \delta_{j,j'-1})$ and $K_{ll'}^\perp = \sum_{i=2}^d K_{l_i,l'_i} \prod_{\tilde{i} \neq i} \delta_{l_i,l'_i}$. (The quantity t corresponds to the sound velocity of a massless phonon and represents the characteristic energy scale of a harmonic lattice; e.g., the bandwidth is given by $2\sqrt{d}t$ for a d -dimensional lattice.) We introduce a set of orthonormal basis functions $\phi_{li}(p_i)$ that satisfy the eigenvalue equation $\sum_{l_i} K_{l_i,l'_i} \phi_{l'_i}(p_i) = U(p_i) \phi_{l_i}(p_i)$, where $U(p_i) = 4t^2 \sin^2 \frac{p_i}{2}$ and $p_i = 2\pi s_i/M_i$. For odd M_i , one may choose $\phi_{li}(p_i) = \sqrt{2/M_i} \sin p_i l_i$ for $s_i = -(M_i - 1)/2, \dots, -1, 1/\sqrt{M_i}$ for $s_i = 0$, and $\sqrt{2/M_i} \cos p_i l_i$ for $s_i = 1, \dots, (M_i - 1)/2$. The basis functions for even M_i are derived to be in an analogous form. The orthonormal basis expressed in product form $\Phi_l(p) = \prod_{i=2}^d \phi_{li}(p_i)$ is a solution of the eigenvalue equation $\sum_{l'} K_{ll'}^\perp \Phi_{l'}(p) = \mathcal{U}(p) \Phi_l(p)$, where $\mathcal{U}(p) = \sum_{i=2}^d U(p_i)$ and $p = (p_2, p_3, \dots, p_d)$. Exploiting this complete orthonormal set, q_{jl} is transformed into

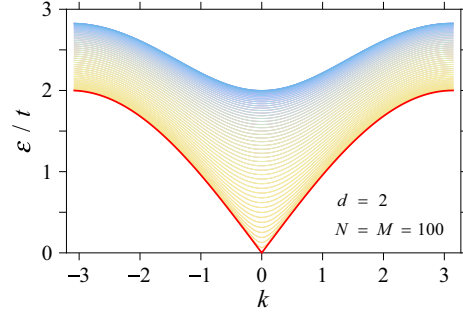


FIG. 1. Energy dispersion for a periodic 2D lattice of $N = M = 100$ in a torus geometry. In this figure, M curves represent eigenenergies for all p as a function of longitudinal wave number k in the first direction. The lowest mode highlighted in red (dark gray) is massless ($p = 0$), while all the other modes are massive ($p \neq 0$).

$\tilde{q}_j(p) = \sum_l q_{jl} \Phi_l(p)$, which follows the equation of motion

$$\ddot{\tilde{q}}_j(p) + \sum_{j'} \tilde{K}_{jj'}(p) \tilde{q}_{j'}(p) = 0, \quad (2)$$

where $\tilde{K}_{jj'}(p) = K_{jj'} + \mathcal{U}(p) \delta_{jj'}$. Note that $\mathcal{U}(p)$ is equivalent to an on-site pinning potential that acts on a 1D harmonic chain. This is also analogous to the mass term μ in the lattice version of the 1D Klein-Gordon equation $\ddot{\psi}_j = \sum_{j'} (\Delta_{jj'} - \mu \delta_{jj'}) \psi_{j'}$, where $\Delta_{jj'}$ denotes the discrete 1D Laplacian. In terms of the transformed variables, the lattice Hamiltonian

$$H = \frac{1}{2} \left(\sum_{jl} \dot{q}_{jl} \dot{q}_{jl} + \sum_{jj'} K_{jj'} q_{jl} q_{j'l'} \right), \quad (3)$$

is rewritten as $H = \sum_p \tilde{H}(p)$ and

$$\tilde{H}(p) = \frac{1}{2} \left[\sum_j \dot{\tilde{q}}_j(p) \dot{\tilde{q}}_j(p) + \sum_{jj'} \tilde{K}_{jj'}(p) \tilde{q}_j(p) \tilde{q}_{j'}(p) \right]. \quad (4)$$

It is easy to see that Eqs. (1) and (2) correspond to the Heisenberg equations of motion for Eqs. (3) and (4), respectively. Thus, the d -dimensional harmonic lattice is reducible to a set of M Klein-Gordon chains. To supplement the argument, the energy dispersion for a periodic 2D lattice in a torus geometry is displayed in Fig. 1, where M curves represent eigenenergies for all p as a function of longitudinal wave number k in the first direction. The lowest mode ($p = 0$) is massless, while all the other modes ($p \neq 0$) are massive. Note that there exists only the massless mode in 1D.

Normally, the system where heat flux is induced is subjected to a temperature bias by connecting at both ends to external heat reservoirs sustained at different temperatures. We consider a Klein-Gordon chain described by the Hamiltonian $\tilde{H}(p)$ connected at both ends to two semi-infinite leads denoted as L and R , which act as external heat reservoirs. At each site of the central system, we assume an equal on-site self-energy Σ ascribed to an inner reservoir, which serves as a temperature probe in the SCR approach. To exclude boundary mismatch, the lead is taken to be a semi-infinite extension of the system, where the same self-energy Σ is incorporated at each site as that in the system. In this

setup, the model describes a finite segment of an infinitely extended Klein-Gordon chain with an equal self-energy at each site. In what follows, each terminal is labeled by $\alpha, \beta \in \{1, 2, \dots, N, L, R\}$, while the index notation $j \in \{1, 2, \dots, N\}$ is used to denote a specific site contained in the system as well as a virtual probe attached to it. For simplicity, it is assumed that a single inner reservoir held at a certain temperature θ_j equally couples to all the mode components, and hence the associated self-energy Σ is mode independent.

The retarded Green's function of a Klein-Gordon chain representing mode p is explicitly written as

$$g_{jj'}(p) = -\frac{e^{-\lambda(p)|j-j'|}}{2t^2 \sinh \lambda(p)}, \quad (5)$$

where $\lambda = -2i \operatorname{sgn}(\varepsilon) \sin^{-1} z$ and $z = \sqrt{\varepsilon^2 - \Sigma - U}/2t$ [18,20]. Note that this two-point correlation function depends only on distance $|j - j'|$ because of lattice translation invariance. We employ the Landauer-Büttiker formula for analyzing thermal transport, which is derived from the quantum Langevin equation formalism [3,4,18] as well as the nonequilibrium Green's function formalism [24–26]. In terms of the Landauer-Büttiker formula, the spectral energy current flowing in terminal α is described by $\tilde{J}_\alpha(p) = \sum_\beta \tilde{G}_{\alpha\beta}(p)(\theta_\alpha - \theta_\beta)$ for a small enough temperature difference $\theta_\alpha - \theta_\beta$. The interterminal thermal conductance is formulated as

$$\tilde{G}_{\alpha\beta}(p) = \frac{1}{2\pi} \int_0^\infty d\varepsilon \frac{\partial f}{\partial \theta} \varepsilon \tilde{T}_{\alpha\beta}(p). \quad (6)$$

Here, $\tilde{T}_{\alpha\beta} = \Gamma_\alpha \Gamma_\beta |g_{\alpha\beta}|^2$ is the transmission coefficient, and $f = (e^{\varepsilon/\theta} - 1)^{-1}$ is the Bose function for phonons. The linewidth function Γ_α is given by $\Gamma = -2 \operatorname{Im} \Sigma$ for $\alpha = j$ and $2t^2 \operatorname{Im} e^{-\lambda}$ for $\alpha = L, R$ [20,27]. Note that in this notation, indices α and β are assigned to the internal sites connected to the relevant terminals for the correlation function $g_{\alpha\beta}$ of the system.

The Landauer-Büttiker equations are solved under the adiabatic condition that no net energy current flows in each inner reservoir, i.e.,

$$J_j = \sum_p \tilde{J}_j(p) = 0. \quad (7)$$

Note that an effective intermode current is allowed to flow via the inner reservoir unless $\tilde{J}_j(p) = 0$ for all p . The local current flowing between two adjacent sites j and $j + 1$ is derived from the related position-velocity correlation function to be $\tilde{J}_{j,j+1}(p) = \sum_\alpha \tilde{G}_{j,j+1}^\alpha(p)(\theta_\alpha - \theta)$ with

$$\tilde{G}_{j,j+1}^\alpha(p) = \frac{1}{2\pi} \int_0^\infty d\varepsilon \frac{\partial f}{\partial \theta} \varepsilon \tilde{T}_{j,j+1}^\alpha(p), \quad (8)$$

and $\tilde{T}_{j,j+1}^\alpha = -2t^2 \Gamma_\alpha \operatorname{Im} g_{j\alpha} g_{j+1,\alpha}^*$, where θ denotes the mean temperature of the system [18]. In terms of energy conservation, the probe and bond currents follow

$$\tilde{J}_j(p) = \tilde{J}_{j,j+1}(p) - \tilde{J}_{j-1,j}(p), \quad (9)$$

and hence the continuity

$$J_{j,j+1} = J_{j-1,j}, \quad (10)$$

of the total bond current $J_{j,j+1} = \sum_p \tilde{J}_{j,j+1}(p)$ results from the adiabatic condition. It is also obvious that $J_{j,j+1} = J_L = -J_R$, where $J_{L,R} = \sum_p \tilde{J}_{L,R}(p)$.

The finite-size thermal conductivity of the d -dimensional system is definable by

$$\kappa = \frac{1}{M} \frac{J_{j,j+1}(N-1)}{\theta_1 - \theta_N}, \quad (11)$$

where $\theta_1 - \theta_N$ is the internal temperature difference [20]. It is easily shown from lattice translation symmetry that a linear temperature profile constitutes a solution for $\tilde{J}_j(p) = 0$ in the limit of $N \rightarrow \infty$ [18,20]. Then, Eq. (11) is reduced to

$$\kappa = \frac{1}{2\pi M} \sum_p \int_0^\infty d\varepsilon \frac{\partial f}{\partial \theta} \varepsilon \tilde{\mathcal{K}}(p), \quad (12)$$

where

$$\tilde{\mathcal{K}}(p) = -\frac{\Gamma \operatorname{Im}[\sinh \lambda(p)]}{4t^2 |\sinh \lambda(p)|^2 \sinh^2 \operatorname{Re} \lambda(p)}. \quad (13)$$

Consequently, the thermal conductivity is formulated as

$$\kappa_d = \frac{1}{2\pi} \int_0^\infty d\varepsilon \frac{\partial f}{\partial \theta} \varepsilon \mathcal{K}_d, \quad (14)$$

in the thermodynamic limit, where

$$\mathcal{K}_d = \frac{1}{(2\pi)^{d-1}} \int_{-\pi}^\pi dp \tilde{\mathcal{K}}(p), \quad (15)$$

for $d \geq 2$ and $\mathcal{K}_1 = \tilde{\mathcal{K}}(0)$ for $d = 1$. In what follows, the dimensionless quantity \mathcal{K}_d is referred to as the thermodynamic transmission in analogy to Eq. (6).

III. NUMERICAL RESULTS AND DISCUSSION

In this section, we elucidate thermal transport in d -dimensional systems coupled to SCRs by using numerical calculations. The previous studies usually assume an Ohmic inner reservoir, for which $\Sigma = -i\gamma\varepsilon$. This corresponds to a simple relaxation time approximation. [The quantity γ refers to the coupling strength, which amounts to the momentum relaxation rate for Ohmic SCRs; see Eq. (16).] In this study, we generalize the self-energy function into the form $\Sigma = -i\gamma\varepsilon^n$ [20]. The exponent n is restricted to odd integers, since $\Sigma(\varepsilon)$ should satisfy the reality condition $\Sigma(\varepsilon) = \Sigma^*(-\varepsilon)$. In the numerical calculations, $n = 3$ is chosen in addition to $n = 1$. It may be worth noting that $\Sigma \propto -i\varepsilon^3\theta$ is derived to second order from perturbation theory for anharmonic three-phonon Umklapp processes at high temperatures. Besides, quenched mass-disorder gives rise to $\Sigma \propto -i\varepsilon^3$ for harmonic linear chains. These analytic results [28] exemplify that nonlinear self-energies are not unphysical.

We begin by discussing the results obtained for $n = 1$. Figure 2 shows probe temperatures derived from numerically solving Eq. (7). As shown in the figure, the numerical results are very similar for $d = 1$ and $d = 2$. The normalized temperature $\Theta_j = (\theta_j - \theta)/(\theta_L - \theta_R)$ varies linearly in the bulk with finite jumps at the boundaries. Recall that the present model is translationally invariant. Therefore, boundary mismatch is not the reason for the observed discontinuities. For a finite system of length N , the internal temperature difference $\Theta_1 - \Theta_N$

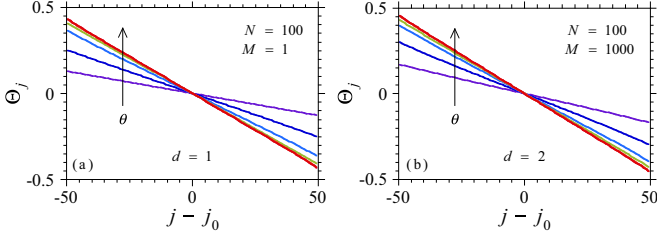


FIG. 2. Probe temperatures derived for $N = 100$, assuming $n = 1$. (a) and (b) show Θ_j in 1D ($M = 1$) and 2D ($M = 1000$), respectively. The reference point $j_0 = (N + 1)/2$ is employed to symmetrize these plots. In the calculation, the coupling strength is taken as $\gamma/t = 0.1$, while the mean temperature is varied as $\theta/t = 10^{-4}, 10^{-3}, \dots, 10^2$.

grows with increasing θ . As $N \rightarrow \infty$, $\Theta_1 - \Theta_N$ tends to approach unity irrespective of θ (not shown).

The spectral energy currents for $d = 2$ are displayed in Fig. 3. The bond current $\hat{J}_{j,j+1}(p)$ concentrates around $p = 0$, indicating that lower modes tend to carry energy current. The probe current $\hat{J}_j(p)$ fully disappears in the bulk of the system. This does not contradict a linear temperature profile as shown in Fig. 2. In the vicinity of the boundaries, $\hat{J}_j(p)$ is negligibly small but nonvanishing, signaling that in a finite-size system, an intermode energy transfer occurs near its boundaries to some extent through the attached inner reservoir. The probe and bond currents are correlated to each other in terms of Eq. (9), which is verified numerically. It is also confirmed that total currents J_j and $J_{j,j+1}$ satisfy Eqs. (7) and (10), respectively.

Figure 4 shows the finite-size thermal conductivity κ in 2D as a function of temperature, in comparison with that in 1D. As seen in the figure, there is no noticeable difference between the numerical results for $N = 100$ and $N = \infty$. This feature implies that Fourier-type transport is retained in the interior of a finite-length system [20]. It is shown in the upper panels that κ approaches its thermodynamic limit κ_2 as $M \rightarrow \infty$. Even for a finite value of M in the range $10 \leq M \leq 1000$,

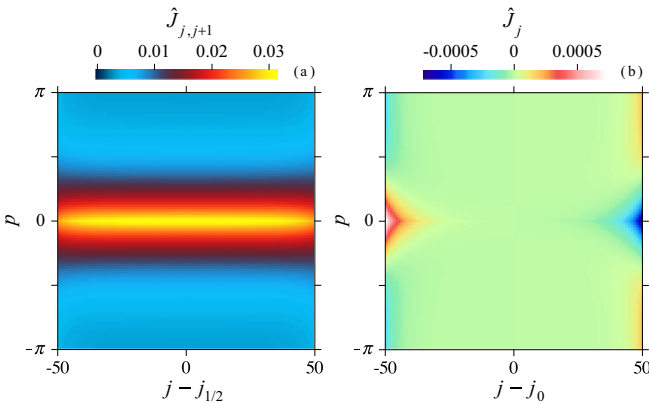


FIG. 3. Normalized spectral energy currents (a) $\hat{J}_{j,j+1}(p) = \hat{J}_{j,j+1}(p)/J_{j,j+1}$ and (b) $\hat{J}_j(p) = \hat{J}_j(p)/J_{j,j+1}$ derived for $d = 2$, assuming $n = 1$. The reference points $j_{1/2} = N/2$ and $j_0 = (N + 1)/2$ are employed to symmetrize these plots. The parameters used in the calculations are $N = M = 100$, $\gamma/t = 0.1$ and $\theta/t = 1$.

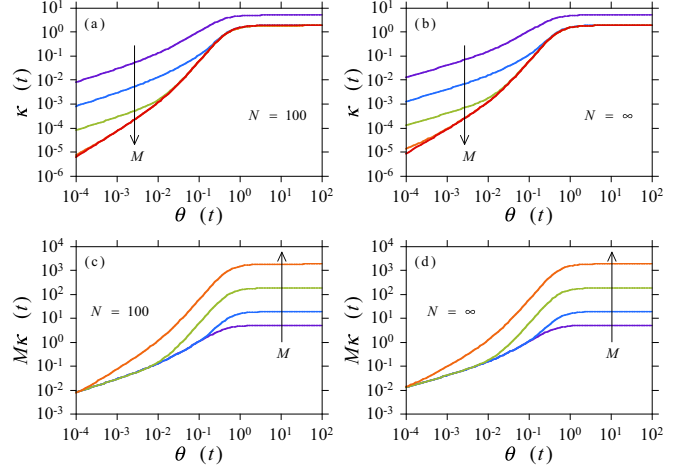


FIG. 4. Finite-size thermal conductivity κ as a function of temperature θ derived for $d = 1, 2$, assuming $n = 1$. Panels (a) and (b), (c) and (d) show κ and $M\kappa$, respectively. The numerical results for $N = 100$ are presented in panels (a) and (c) in comparison to those for $N = \infty$ in panels (b) and (d). The coupling strength is taken as $\gamma/t = 0.1$, while the lateral size is varied as $M = 1, 10, 100, 1000, \infty$ in panels (a) and (b) and $M = 1, 10, 100, 1000$ in panels (c) and (d). Note that $M = 1$ corresponds to $d = 1$.

κ is very close to κ_2 at high enough temperatures. In the low-temperature regime, however, κ and κ_1 exhibit a similar temperature dependence, which is distinct from that shown by κ_2 . Thus, 1D-to-2D crossover of thermal transport depends on not only lateral size but also temperature. The temperature-dependent crossover is more quantitatively examined in the lower panels, where the product $M\kappa$ is shown. For all the 2D systems of finite lateral sizes, this quantity converges to κ_1 at low enough temperatures. This is an expected result, since energy current in such a finite system is carried only by the lowest mode ($p = 0$) in the low-temperature limit. Similar features are observed in 1D-to-3D crossover (not shown).

Figure 5 summarizes the thermal conductivity κ_d and the associated transmission \mathcal{K}_d in the thermodynamic limit derived for various d . Generally, κ_d increases with temperature until reaching its classical limit. A finite value of κ_d is indicative of normal heat transport. Following Bonetto *et al.* [16], the classical limit is evaluated for $n = 1$ to be $\kappa_{cl} = t^2/2\gamma$ in 1D, $(1 - 2/\pi)\kappa_{cl}$ in 2D, and $0.210\kappa_{cl}$ in 3D. These theoretical predictions agree with the numerical results. In the low-temperature regime, the conductivity behaves as $\kappa_d \propto \gamma^{d/2-1}\theta^{d/2}$, indicating that κ_1 decreases with the coupling strength γ , κ_2 is independent of γ , and κ_3 increases with γ . The latter two behaviors, which differ from those observed in the classical limit, are unusual, given that γ represents the momentum relaxation rate for $n = 1$. Naturally, the temperature dependence of κ_d reflects the energy dependence of \mathcal{K}_d . As shown in the figure, the thermodynamic transmission varies as $\mathcal{K}_d \propto (\gamma\varepsilon)^{d/2-1}$ in the low-energy regime.

The numerical results obtained for $n = 3$ is quite different from those for $n = 1$, as shown in Fig. 6. For $n = 3$, the thermodynamic transmission behaves as $\mathcal{K}_d \propto \gamma^{-1}\varepsilon^{d-3}$ in the low-energy regime. In this case, the thermal conductivity κ_d is divergent and thereby transport is anomalous for $d \leq 2$.

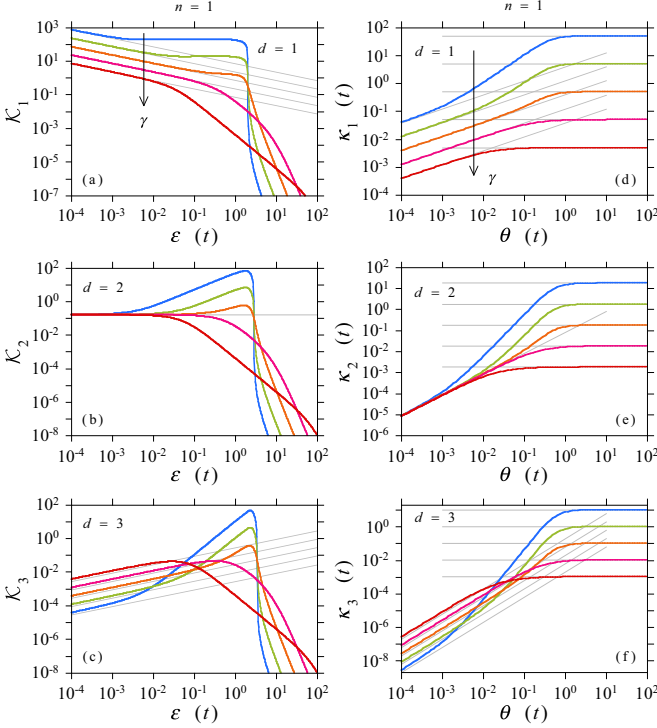


FIG. 5. (a)–(c) Thermodynamic transmission \mathcal{K}_d as a function of energy ε and (d)–(f) thermal conductivity κ_d as a function of temperature θ derived for $d = 1, 2, 3$, assuming $n = 1$. In each plot, the coupling strength is varied as $\gamma/t = 10^{-2}, 10^{-1}, \dots, 10^2$. The thin gray lines show the analytical results in the low- ε limit, in the low- θ limit, and in the high- θ limit.

It is observed in the numerical calculation that the finite-size conductivity exhibits the power-law divergence $\kappa \propto N^{1/2}$ in 1D and the logarithmic divergence $\kappa \propto \ln N$ in 2D (not shown). Interestingly, these asymptotic behaviors are typical of low-dimensional nonlinear or disordered lattices [1–4]. However, a finite value of κ_3 shown in the figure indicates that normal transport is recovered for $d = 3$. In 3D, the thermal conductivity varies as $\kappa_3 \propto \gamma^{-1}\theta$ at low temperatures.

As demonstrated above, whether the anomaly in thermal transport disappears or emerges depends on the exponent n as well as the dimension d . To explore its physical implications, we first address the kinetic aspects of the present SCR model. The total linear momentum is expressed as $P = \sum_{j,l} \dot{q}_{jl} = \sqrt{M} \sum_j \dot{\tilde{q}}_j(0)$ in terms of the transformed variables. Thus, P correlates only to the lowest mode $p = 0$ regardless of d . It is shown from the relevant 1D quantum Langevin equation [20] that P obeys the differential equation

$$\dot{P} + (-1)^{(n-1)/2} \gamma P^{(n-1)} = 0, \quad (16)$$

where $P^{(n)}$ denotes the n th derivative of P with respect to time (do not confuse this with the n th power of P). In terms of Eq. (16), one finds that the conservation law for P is broken by coupling to SCRs for $n = 1$, whereas P remains a conserved quantity for $n = 3, 5, 7, \dots$. Assuming a plane wave solution $\tilde{q}_j(0) \propto e^{i(kj - \varepsilon t)}$, the Langevin equation leads to the dispersion relation $k = (i\gamma\varepsilon)^{1/2}/t$ for $n = 1$ and ε/t for $n = 3, 5, 7, \dots$ in the low-frequency and long-wavelength limit.

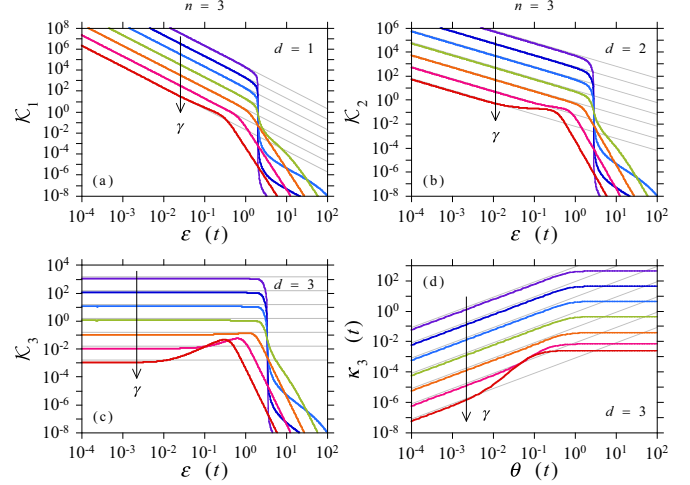


FIG. 6. (a)–(c) Thermodynamic transmission \mathcal{K}_d as a function of energy ε derived for $d = 1, 2, 3$, assuming $n = 3$. The associated thermal conductivity κ_d is divergent in 1D and 2D, while κ_3 remains finite as demonstrated in panel (d), which shows κ_3 as a function of temperature θ . In each plot, the coupling strength is varied as $\gamma t = 10^{-4}, 10^{-3}, \dots, 10^2$. The thin gray lines show the analytical results in the low- ε limit and in the low- θ limit.

This indicates that the propagating mode with no excitation gap no longer exists for $n = 1$, whereas it remains intact for $n = 3, 5, 7, \dots$. In the light of these arguments, the observations for $d \leq 2$ imply that thermal transport in low dimensions becomes normal by violating total momentum conservation to eliminate the massless mode, whereas anomalous transport occurs when total momentum is conserved and the massless mode persists.

Although the generic argument given above is instructive for thermal transport in low dimensions, it does not account for how dimensional crossover takes place. To solve this problem, a more quantitative analysis proceeds as follows. The thermodynamic transmission \mathcal{K}_d is given by integrating the spectral transmission $\tilde{\mathcal{K}}(p)$ over the $d - 1$ -dimensional p space. Note that the p dependence arises from the mass term $\mathcal{U}(p) = \sum_{i=2}^d U(p_i)$ contained in the equation of motion. As shown in Fig. 7, $\tilde{\mathcal{K}}(p)$ behaves as $\tilde{\mathcal{K}}(0)\theta(\varepsilon - \varepsilon_U)$, where $\theta(x)$ denotes the Heaviside step function. The cutoff energy is given in the $\mathcal{U} \rightarrow 0$ limit by $\varepsilon_U = 2\mathcal{U}/\gamma$ for $n = 1$ and $\sqrt{\mathcal{U}}$ for $n = 3, 5, 7, \dots$. These expressions are implied from the renormalized variable z in the Green's function. Thus, the thermodynamic transmission can be recast into the form $\mathcal{K}_d = \tilde{\mathcal{K}}(0)\mathcal{J}_d$. Changing variables from p_i to $u_i = U(p_i)/4t^2$, we obtain

$$\mathcal{J}_d = \frac{1}{\pi^{d-1}} \int_0^1 \prod_{i=2}^d du_i \frac{\theta(b - \sum_{i=2}^d u_i)}{\sqrt{\prod_{i=2}^d u_i(1 - u_i)}} \simeq \frac{(b/\pi)^{(d-1)/2}}{\Gamma[(d+1)/2]}, \quad (17)$$

where $\Gamma(x)$ denotes the gamma function, and $b = \gamma\varepsilon/8t^2$ for $n = 1$ and $\varepsilon^2/4t^2$ for $n = 3, 5, 7, \dots$. In performing the multiple integration in Eq. (17), we assumed $b \ll 1$. This condition is verifiable in the $\varepsilon \rightarrow 0$ limit. In this limit, $\tilde{\mathcal{K}}(0) = t/(2\gamma\varepsilon)^{1/2}$ for $n = 1$ and $2t/\gamma\varepsilon^{n-1}$ for $n = 3, 5, 7, \dots$

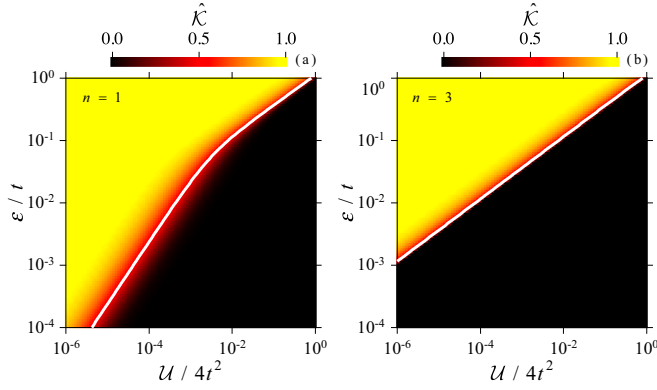


FIG. 7. Normalized spectral transmission $\hat{\mathcal{K}}(p) = \tilde{\mathcal{K}}(p)/\tilde{\mathcal{K}}(0)$ as a function of $\mathcal{U}(p)$ and ε calculated for (a) $n = 1$ and (b) $n = 3$. In the calculation, the coupling strength is taken as $\gamma = 0.1$ in units where $t = 1$. The solid line inserted in the figure indicates a critical point where $\hat{\mathcal{K}}(p) = 1/2$.

Hence, we arrive at the low-energy approximations $\mathcal{K}_d \propto (\gamma\varepsilon)^{d/2-1}$ for $n = 1$ and $\gamma^{-1}\varepsilon^{d-n}$ for $n = 3, 5, 7, \dots$. These analytical results agree well with the numerical results. (In the high-energy regime, \mathcal{K}_d is not analytically evaluated. However, this is irrelevant to finiteness or divergence of κ_d .) Furthermore, the thermal conductivity defined by Eq. (14) is analytically calculated to be $\kappa_d \propto I_{d/2-1}\gamma^{d/2-1}\theta^{d/2}$ for $n = 1$ and $I_{d-n}\gamma^{-1}\theta^{d-n+1}$ for $n = 3, 5, 7, \dots$, where $I_\nu = \int_0^\infty dx e^x x^{\nu+2}/(e^x - 1)^2$. Note that I_ν diverges for $\nu \leq -1$. Again, these theoretical results coincide quantitatively with the numerical results at low temperatures. Note that both peculiar behaviors in high dimensions for $n = 1$ and anomalous transport in low dimensions for $n = 3$ are accounted for in a unifying manner in terms of the energy cutoff depending on n .

These arguments for thermal transport in the d -dimensional quantum model can be summarized as follows.

For $n = 1$, total momentum conservation is broken and the massless mode is eliminated. In this case, κ_d remains finite and normal transport occurs for an arbitrary value of d . For $n = 3, 5, 7, \dots$, however, total momentum is conserved and the massless mode is sustained. In this case, κ_d diverges and thermal transport becomes anomalous as long as $d < n$, whereas normal transport is recovered when $d \geq n$. Note that these criteria are inviolate even in the case of $n = 1$.

IV. SUMMARY

We have investigated thermal transport in d -dimensional quantum harmonic lattices in contact with SCRs. An orthogonal transformation enables us to treat the d -dimensional system as a set of Klein-Gordon chains. For generality, the self-energy due to SCR is assumed in the form $\Sigma = -i\gamma\varepsilon^n$, where n is an odd integer. For $n = 1$, total momentum conservation is violated and the massless mode vanishes. In this case, thermal conductivity remains finite in the thermodynamic limit and normal transport takes place for an arbitrary value of d . For $n = 3, 5, 7, \dots$, however, total momentum is conserved and the massless mode remains intact. In this case, thermal conductivity diverges and thermal transport becomes anomalous as long as $d < n$, whereas normal transport is recovered when $d \geq n$. These criteria derived for quantum-mechanical lattices imply that normal transport emerges in high enough dimensions despite total momentum conservation, and reinforce the prevailing conjecture deduced in the classical limit.

ACKNOWLEDGMENT

This work was supported by a Grant-in-Aid for Scientific Research (Grant No. 18K03977) from the Japan Society for the Promotion of Science.

-
- [1] F. Bonetto, J. L. Lebowitz, and L. Rey-Bellet, in *Mathematical Physics 2000*, edited by A. Fokas, A. Grigoryan, T. Kibble, and B. Zegarlinski (Imperial College Press, London, 2000), pp. 128–150.
 - [2] S. Lepri, R. Livi, and A. Politi, *Phys. Rep.* **377**, 1 (2003).
 - [3] A. Dhar, *Adv. Phys.* **57**, 457 (2008).
 - [4] S. Lepri (ed.), *Thermal Transport in Low Dimensions* (Springer, Heidelberg, 2016).
 - [5] T. Prosen and D. K. Campbell, *Phys. Rev. Lett.* **84**, 2857 (2000).
 - [6] C. W. Chang, D. Okawa, H. Garcia, A. Majumdar, and A. Zettl, *Phys. Rev. Lett.* **101**, 075903 (2008).
 - [7] X. Xu, L. F. C. Pereira, Y. Wang, J. Wu, K. Zhang, X. Zhao, S. Bae, C. T. Bui, R. Xie, J. T. L. Thong, B. H. Hong, K. P. Loh, D. Donadio, B. Li, and B. Özyilmaz, *Nat. Commun.* **5**, 3689 (2014).
 - [8] S. Ghosh, W. Bao, D. L. Nika, S. Subrina, E. P. Pokatilov, C. N. Lau, and A. A. Balandin, *Nat. Mater.* **9**, 555 (2010).
 - [9] A. Dhar, *Phys. Rev. Lett.* **86**, 5882 (2001).
 - [10] B. Ash, A. Amir, Y. Bar-Sinai, Y. Oreg, and Y. Imry, *Phys. Rev. B* **101**, 121403(R) (2020).
 - [11] M. Büttiker, *Phys. Rev. B* **33**, 3020 (1986).
 - [12] S. Datta, *Electronic Transport in Mesoscopic Systems* (Cambridge University Press, Cambridge, 1995).
 - [13] Y. Imry, *Introduction to Mesoscopic Physics* (Oxford University Press, New York, 2008).
 - [14] M. Bolsterli, M. Rich, and W. M. Visscher, *Phys. Rev. A* **1**, 1086 (1970).
 - [15] M. Rich and W. M. Visscher, *Phys. Rev. B* **11**, 2164 (1975).
 - [16] F. Bonetto, J. L. Lebowitz, and J. Lukkarinen, *J. Stat. Phys.* **116**, 783 (2004).
 - [17] W. M. Visscher and M. Rich, *Phys. Rev. A* **12**, 675 (1975).
 - [18] A. Dhar and D. Roy, *J. Stat. Phys.* **125**, 801 (2006).
 - [19] D. Roy, *Phys. Rev. E* **77**, 062102 (2008).
 - [20] K. Hattori and M. Yoshikawa, *Phys. Rev. E* **99**, 062104 (2019).
 - [21] H. Nakazawa, *Prog. Theor. Phys.* **39**, 236 (1968).

- [22] H. Nakazawa, *Prog. Theor. Phys. Suppl.* **45**, 231 (1970).
- [23] D. Roy and A. Dhar, *J. Stat. Phys.* **131**, 535 (2008).
- [24] T. Yamamoto and K. Watanabe, *Phys. Rev. Lett.* **96**, 255503 (2006).
- [25] J.-S. Wang, J. Wang, and J. T. Lü, *Eur. Phys. J. B* **62**, 381 (2008).
- [26] S. G. Das and A. Dhar, *Eur. Phys. J. B* **85**, 372 (2012).
- [27] K. Hattori and Y. Nakamura, *Phys. Rev. B* **97**, 224312 (2018).
- [28] G. P. Srivastava, *The Physics of Phonons* (Taylor and Francis, New York, 1990).